18

Customized Heart Check System by Using Integrated Information of Electrocardiogram and Plethysmogram Outside the Driver's Awareness from an Automobile Steering Wheel

Motohisa Osaka
Nippon Veterinary and Life Science University, Japan

1. Introduction

1.1 Sudden cardiac death of drivers

The annual number of sudden cardiac deaths is increasing in Japan, and is estimated to be more than 50,000 on the basis of findings from the multicenter research group (Toyoshima et al., 1996). In the United States, sudden cardiac death is the greatest cause of natural death, causing more than 400,000 adult fatalities each year (Zipes & Wellens, 1998) and it is the most common lethal manifestation of heart disease (Bauer et al., 2006). The high incidence makes sudden cardiac death a major challenge in public health. In most cases, the mechanism is abrupt occurrence of ventricular tachyarrhythmia, rapidly progressing to ventricular fibrillation and causing cardiac pump failure with unconsciousness. It is supposed that sudden cardiac death sometimes occurs while the subject is driving an automobile. A Japanese newspaper (March 29, 2010) reported, "While a bus driver (65 years old) was driving a bus, he suffered severe chest pain and gave up steering so that the bus ran in a zigzag and crashed into a wall to be on fire. " Although such cases can easily be found on web sites, there has been little reported study. Lam and Lam reported that among older drivers aged 60 or above in New South Wales, Australia from 1996 to 2000, 409 (1.1%) of 36,595 were recognized as having suffered a sudden illness immediately prior to a crash, and that 254 (0.7%) of those episodes resulted in the driver's death and injury in the crash (Lam & Lam, 2005). According to "Suicide and Natural Deaths in Road Traffic — Review" from Accident Research Centre of Monash University, the percentages of natural driver deaths out of all vehicle deaths were reported to vary from 0.2% to 19% in 10 studies (Routely et al., 2003). The Review listed 19 studies in total in the Appendix. It was reported that the percentages of cardiovascular disease in drivers who met natural deaths were from 68% to 97%. We speculated, on examination of a summary of those studies, that the total number of natural driver deaths and the number of natural driver deaths due to cardiac events were, respectively, 5 -10% and about 5% as percentages of all vehicle deaths. There may also be cases in which a patient receives a warning from his own heart of imminent sudden cardiac death, and is able to survive, or at least to prevent injury to others.

1.2 Is there any precursor of sudden cardiac death?

Is it possible to predict sudden cardiac death a few hours in advance of its occurrence? The mechanism is abrupt occurrence of ventricular tachyarrhythmia or complete atrioventricular block. It was noted on analyses of ambulatory 24-hour electrocardiogram recordings (Holter recordings) that some measures of heart rate variability may change about 1 hour before the onset of sustained or nonsustained ventricular tachycardia (Huikuri et al., 1993). No reliable precursor of sudden cardiac death, however, had yet been discovered.

Muller et al. reported that there were two peaks of the frequency of circadian variation of sudden cardiac death at 11 am and 6 pm (Muller et al., 1987). Particularly, the highest peak was about 3 hours after awakening. These results suggested that there might be the relationship between the occurrence of sudden cardiac death and the intrinsic circadian rhythm of autonomic nervous system and/or endocrine system. We analyzed ambulatory 24-hour electrocardiogram (ECG) recordings of 24 patients who were hospitalized due to leg fracture. We calculated the low-frequency component (LF: 0.04-0.15Hz), the high-frequency component (HF: 0.15-0.4Hz) of RR intervals (ms), and the ratio LF/HF, which are recognized as measures of combined sympathetic and parasympathetic activity,

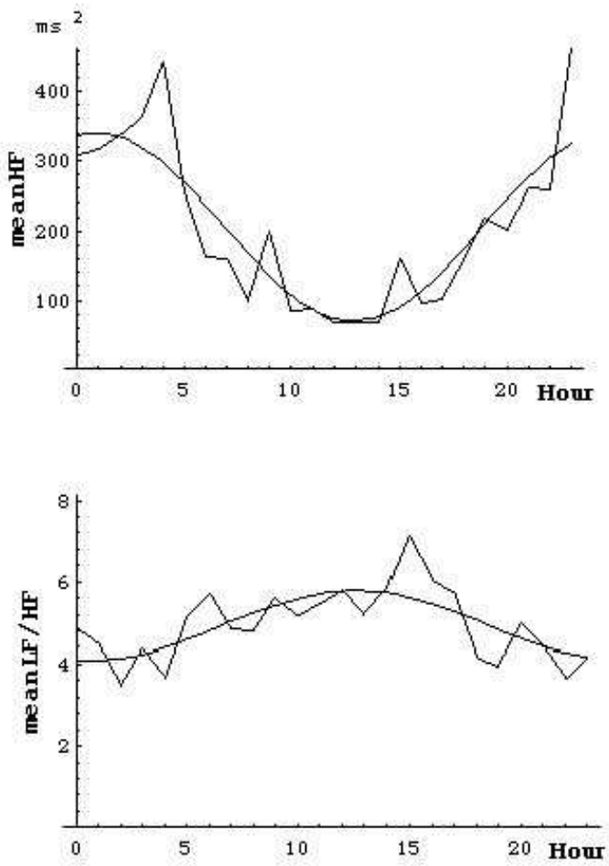

Fig. 1. Circadian variation of autonomic activity. LF (unit, ms^2), the low-frequency component of RR intervals (ms); HF (unit, ms^2), the high frequency component; LF/HF (no unit), the ratio of LF to HF.

parasympathetic activity, and sympathetic activity, respectively (Berger et al., 1989; Osaka et al., 1993; Task Force of the European Society of Cardiology and the North American Society of Pacing and Electrophysiology, 1996). Since those patients were lying still on bed during the recordings, the variations of HF and LF/HF represents intrinsic circadian rhythm of parasympathetic and sympathetic activity, respectively. Figure 1 shows that the peak of LF/HF and the nadir of HF are around noon, and that the increase of LF/HF and the decrease of HF begin around awakening. Thus, these findings suggest that the predominance of sympathetic activity over parasympathetic activity may trigger the cardiac event about 3 hours after awakening.

Experimentally, Schwartz et al. demonstrated that autonomic stress could trigger lethal ventricular arrhythmias in dogs with myocardial infarction (Schwartz et al., 1988). Their observation was made in an animal model for sudden cardiac death. According to their article, dogs with healed anterior myocardial infarctions perform an exercise stress test, toward the end of which a 2-minute myocardial ischemia is created by occluding the left circumflex coronary artery. This clinically relevant combination of transient myocardial ischemia at the time of physiologically elevated sympathetic activity results in ventricular fibrillation in almost 60 per cent of the animals. The outcome during the exercise and ischemia test identifies and defines two groups of animals according to the occurrence of ventricular fibrillation or survival –"susceptible" and "resistant", respectively. Although the former group tends to show a further increase in the already elevated heart rate, the latter group tends to show a decrease. This heart rate reduction is prevented by atropine and clearly reveals the presence of powerful vagal reflexes. Such a behavior of heart rate could be taken to suggest the presence of a relative sympathetic dominance among susceptible animals and of a relative parasympasthetic dominance among resistant animals.

Clinically, analysis of Holter recordings was the basis for our previous report that heart rate and LF/HF increase steadily with the decrease of HF from 45 minutes before the onset of nonsustained ventricular tachycardia until the actual onset (Osaka et al., 1996). This suggested that increased sympathetic activity and decreased parasympathetic activity may trigger nonsustained ventricular tachycardia, and also indicated that trends in autonomic activity may be useful for detecting any precursor of a cardiac event that is triggered or worsened by autonomic imbalance.

It has been known for some time that the power spectra of heart rate from healthy individuals exhibit a *1/f*-like pattern ($Power = C f^{b}$, where $b \approx -1$ and C is a proportionality constant) in the low-frequency range ($f < 0.1$Hz) (Kobayashi & Musha, 1982; Peng et al., 1993). This is reflected in the fractal nature of HR. Loss of multifractality is closely correlated with prognosis and severity of heart disease (Ivanov et al., 1999). Hence, we presumed that the low-frequency component would be strongly correlated with prognosis. Experimentally, we showed that sympathetic activity strongly correlates with heart rate and blood pressure at both 0.05Hz and 0.80Hz in conscious rats and that this correlation is baroreflex-independent (Sakata et al., 2002). This was consistent with the finding that that the low-frequency component (<0.1Hz) of the transfer function between blood pressure and heart rate is baroreflex-independent in normotensive humans (Taylor & Eckberg, 1996). Hence, we presumed that the low-frequency component of sympathetic activity may play a key role in triggering lethal tachyarrhythmias, and that characteristic changes in sympathetic activity might occur before a cardiac event.

1.3 V-shaped trough in autonomic activity as a possible precursor

We aimed at finding a consistent precursor of a lethal cardiac event by examining Holter recordings in which such a spontaneous event was recorded. Holter recordings of 34 patients experiencing a cardiac event (Event-group, 20 deaths) were compared with 191 controls (NoEvent-group) (Osaka et al., 2010). The Event-group included 25 patients with ventricular fibrillation or acute myocardial infarction, and 9 with cardiac arrest due to complete atrioventricular block. We calculated logarithms of the moving average of 5 successive values for the low-frequency component (LF), the high-frequency component (HF), and the ratio LF/HF of heart rate variability: ln(LF), ln(HF) and ln(LF/HF). A V-shaped trough appeared in the curve of ln(LF/HF) [sV-trough] or ln(HF) [pV-trough] before such an event in 31 patients of the Event-group. The V-trough was marked by a small variation lasting 2 hours, an abrupt descent lasting 30 minutes, and a sharp ascent for 40 minutes. Figure 2a-e shows a representative case in the Event-group. The patient (male, 72 years old) suffered from acute myocardial infarction and died of ventricular fibrillation during the recording. Figure 2a shows progression from regular sinus rhythm to ventricular fibrillation with sporadic short runs of ventricular tachycardia. In Figure 2b sustained ST elevation appears at 21:50, indicating the occurrence of acute myocardial infarction. It is noted that thereafter slow oscillations of HR seem to disappear with their variability depressed (Figure 2c). The variation of ln(LF/HF) decreases from 20:00 to 22:00, and lies approximately within the mean±SD which was calculated as described below (Figure 2d). This decrease appears before ST elevation. Next, ln(LF/HF) falls steeply and then rises sharply. Figure 2d shows a V-shaped trough in sympathetic activity, which is referred to subsequently in the manuscript simply as "V-trough." Although such a sharp rise of ln(LF/HF) and a simultaneous decrease of ln(HF) (Figure 2e) would normally be expected to accompany an increase of HR, there is instead a decrease in heart rate which is accompanied by a reduction in variability (Figure 2c). Slow ventricular tachycardia appeared at 0:30 and ceased at 0:50, then ventricular fibrillation appeared at 1:27 terminating in cardiac standstill at 1:55 (data not shown).

Figure 3a-d shows another representative case in the Event-group. The patient (male, 74 years old) suffered from complete atrioventricular block and died during the recording. ST elevation appeared at 10:56, indicating the occurrence of acute myocardial infarction. Figure 3a shows that complete atrioventricular block, which was induced by acute myocardial infarction, causes a compensatory atrioventricular rhythm at 11:00 and finally, cardiac arrest at 11:10. Heart rate decreases during sleep from 23:00 to 6:00 (Figure 3b). The variation of ln(HF) decreases from 2:00 to 4:00, which is approximately within the mean±SD (Figure 3c). Then ln(HF) declines quickly, but suddenly reverses direction and shows a striking increase, although it might normally be expected to fall after rising so abruptly. These changes are characteristic of a V-trough in parasympathetic activity. In spite of the predominance of changes in ln(HF) as compared with ln(LF/HF), heart rate increases abruptly at 7:20, and fails to react normally to the predominance of parasympathetic activity vs. sympathetic activity.

From the finding that a V-shaped trough was observed preceding the event in almost all patients of the Event-group, we defined the criteria for a V-trough in sympathetic activity (sV-trough) as indicated in Figure 4. To characterize the time series of ln(LF/HF), we calculated the mean±SD of consecutive values of ln(LF/HF), which corresponded to a

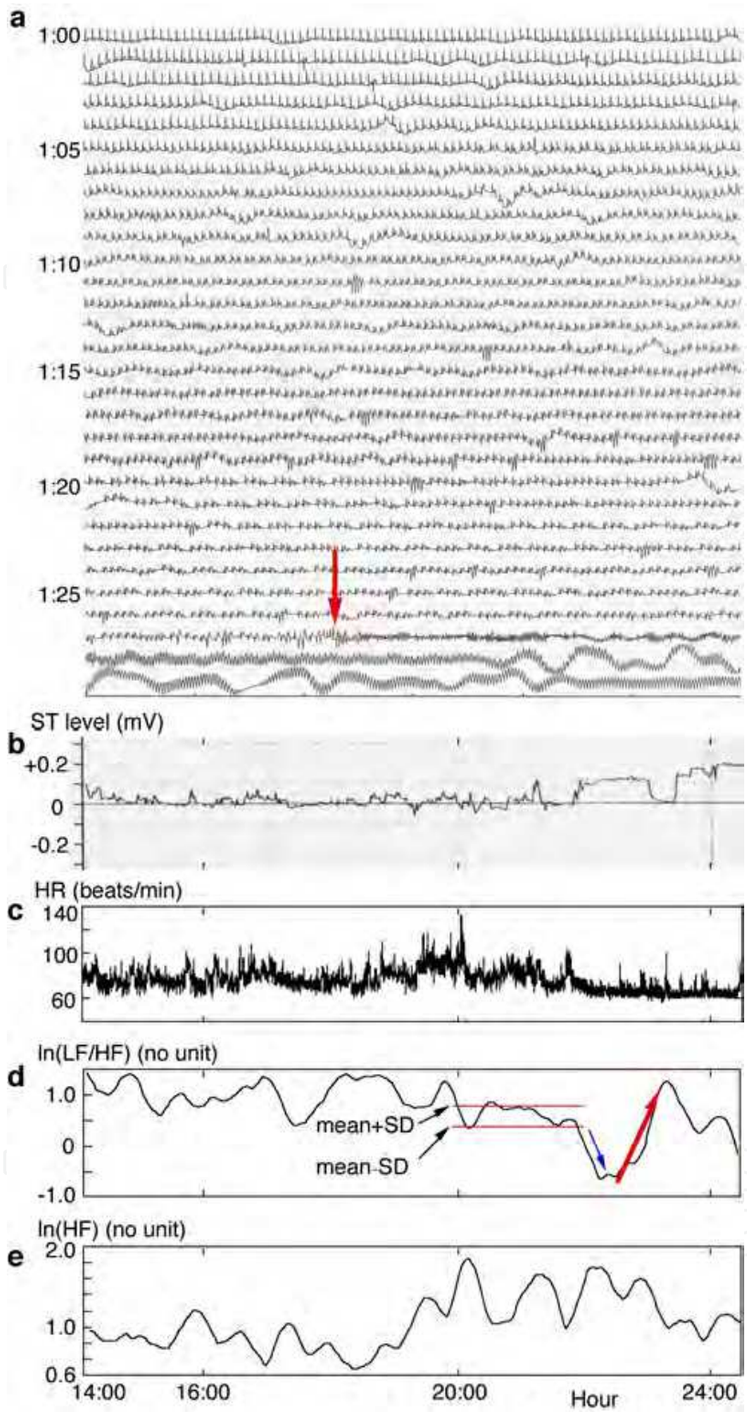

a. Holter recording before the occurrence of ventricular fibrillation (starting from the red arrow). b. ST level up to the time of onset of slow ventricular tachycardia (0:30). c. Tachogram of heart rate (HR). d. Tachogram of the logarithm of the ratio of the low-frequency component to the high-frequency component, ln(LF/HF). The two red horizontal lines represent mean±SD for 120 minutes. e. Tachogram of the logarithm of the high-frequency component, ln(HF). From (Osaka et al., 2010).

Fig. 2. V-trough of sympathetic activity in a representative case from the Event-group.

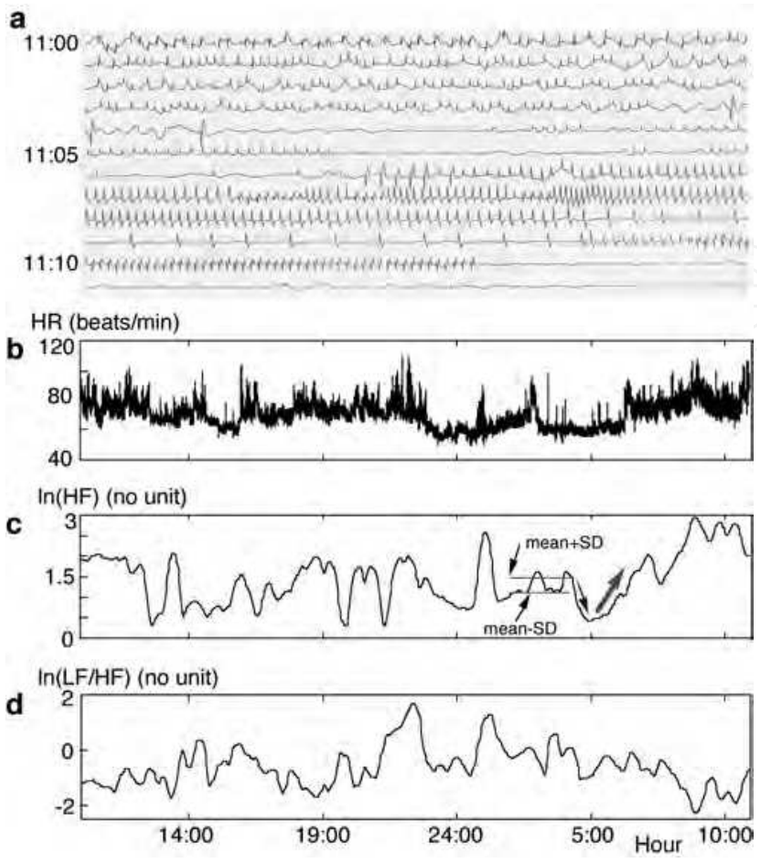

a. Holter recording displaying a compensatory atrioventricular rhythm which is induced by complete atrioventricular block at 11:00, followed by cardiac arrest. b. Tachogram of heart rate (HR). c. Tachogram of ln(HF). d. Tachogram of ln(LF/HF). From (Osaka et al., 2010).

Fig. 3. V-trough of parasympathetic activity in a representative case from the Event-group.

baseline period of 120 min. The criteria included four necessary conditions, the first that ln(LF/HF) fluctuate approximately within a narrow range between mean±SD for 120 minutes, and the second that ln(LF/HF) must increase sharply for a period of 40 minutes (ascent period) after an abrupt descent lasting 30 minutes (descent period). These necessary conditions were as follows:

R is defined as (mean + SD) of ln(LF/HF) in each of the consecutive baseline periods (Figure 4). Slope 1 is defined as a slope of 3SD of ln(LF/HF) per the baseline period of BL minutes (BL = 120). Slope 2 is defined as a slope of a straight line fitted into values of ln(LF/HF) during the ascent period.

T is defined as total time, in which mean – SD ≤ ln(LF/HF) ≤ mean + SD.

Figure 4 shows such an example that $T = T_1 + T_2 + T_3$.

Necessary condition 1: If $R \geq 1.5$, $T \geq BL \times (3/4)$ min, and if not, $T \geq BL \times (2/3)$ min.

Necessary condition 2: Slope 2 > Slope 1.

Necessary condition 3: The lower end of Slope 2 < mean – 3SD.

Necessary condition 4: HR decreases, while ln(LF/HF) increases sharply for a period of 40 minutes.

It may be noted that larger values of mean and SD for ln(LF/HF) are associated with stricter conditions (Figure 4). V-troughs of ln(HF) were used in place of ln(LF/HF) as an index of parasympathetic activity (pV-trough). The necessary condition 4 was also replaced with that HR increases, while ln(HF) increases sharply for a period of 40 minutes. We examined all the recordings automatically using this algorithm. An sV-trough was observed in 22 patients before the onset of ventricular fibrillation or acute myocardial infarction. A pV-trough was observed in all 9 patients before the onset of complete atrioventricular block. In the NoEvent-group, an sV-trough and a pV-trough were observed in 10 (5%) and 20 (10%) subjects, respectively. The positive predictive accuracy of an sV-trough for ventricular fibrillation or acute myocardial infarction and that of a pV-trough for complete atrioventricular block was 88% and 100%, respectively. We reported that the hemodynamics consisting of heart rate, sympathetic activity and blood pressure is modeled excellently by modification of a known chaotic electrical circuit, Chua circuit (Osaka & Watanabe, 2004). A V-trough of sympathetic activity appears by increasing the resistive element between sympathetic activity and blood pressure in the circuit, which corresponds to the impaired regulation of blood pressure by sympathetic activity (Osaka, in press). This finding is consistent with an acknowledged finding that the depressed baroreflex (reflex of blood pressure by sympathetic activity) may trigger a lethal arrhythmia (Schwartz et al., 1988).

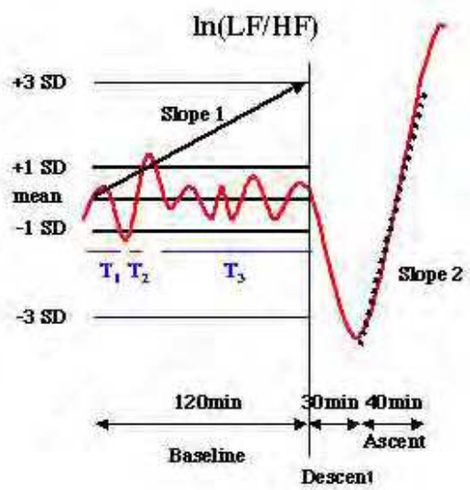

Fig. 4. Criteria for V-trough of ln(LF/HF). From (Osaka et al., 2010).

2. Recording of ECG outside the driver's awareness

2.1 Inevitable noise of ECG

Although there were some trials monitoring the ECG of drivers (Jeong et al., 2007), no automobile equipped with such a system has never been marketed, as a result of the fact that the ECG was largely contaminated by noise. Therefore, we developed new electrodes for installation on a steering wheel, through which an ECG limb lead could be recorded with suppression of noise (Osaka et al., 2008). However, some artifacts were still present as a result of the physical movements accompanying the handling of a steering wheel and as a result of jolts due to road conditions. Such artifacts are inevitable, because drivers sitting in the driver's seat do not remain still, as they might during the recording of a standard ECG. At the present time we have not yet succeeded in recording the entire PQRST pattern of waves in ECG from a

steering wheel (steering-ECG), because of contamination of the baseline by noise. Therefore, the first half of our goals for recording the steering-ECG were in the following: i) confirmation of correctness of steering-ECG, ii) confirmation of correctness of RR intervals of steering-ECG, iii) confirmation of correctness of heart rate variability analysis of steering-ECG, when a driver remains still with gripping a steering wheel by both hands. However, noise unavoidably contaminates the steering-ECG, because the driver is not lying on the bed calmly but is handling the steering wheel. Although an ECG from a chest lead (chest-ECG) was recorded simultaneously as a reference in order to examine the correctness of the steering-ECG, the chest-ECG was also unavoidably contaminated. Hence, it was impossible to continuously find a one-to-one correspondence between the R waves of a steering-ECG and those of a chest-ECG. However, it was possible to observe fluctuations of heart rate variability by neglecting those inevitable artifacts. The second half of our goals was thus to evaluate the fluctuation of autonomic nervous activity from the heart rate variability analysis of steering-ECG in spite of noise. We examined whether fluctuations of sympathetic and parasympathetic nervous activities measured from steering-ECG were consistent with those from chest-ECG.

2.2 Methods for steering-ECG

2.2.1 Subjects

We simultaneously recorded the ECG from a chest lead and, separately, from a steering wheel in each of 10 normal subjects driving an automobile for 90 minutes. Then, the subjects sitting in the driver's seat remained still with gripping a steering wheel by both hands during the first minute of the recording.

2.2.2 Steering wheel

We refurbished the steering wheel of an automobile that was on sale by installing a pair of electrodes around the grip site on each side (Figure 5). One electrode of the right pair was a (-) electrode, and the other, an indifferent electrode. One electrode of the left pair was a (+) electrode, and the other, an indifferent electrode. From these electrodes we made ECG recordings which corresponded to the standard ECG of lead I. The electric wires from the installed electrodes were connected to a signal amplifier set up in the front portion of the automobile through a spiral cable within the steering wheel. We carefully kept the horn and an air bag intact for safety purposes. The recorded signals were 1~5mV. These signals were amplified 1,700 times. A bandpass-filter of 0.2~35Hz was used to remove noise. With an AD converter, the signals from the steering wheel lead were sampled at 200Hz. We consecutively searched the R waves of the steering-ECG and chest-ECG visually on a screen. We examined whether the R waves of the steering-ECG corresponded in a regular one-to-one fashion with the R waves of the chest-ECG. The R waves that did correspond to each other in this way were represented as {steering-R_k} and {chest-R_k}. Intervals of {steering-R_k} and {chest-R_k} ({steering-RR_k} and {chest-RR_k}) were measured as the intervals of the QRS waves at a threshold level. The threshold level was manually determined for each record. {steering-RR_k} were compared with {chest-RR_k} to identify errors due to the filtering of steering-ECG. Since each element of {steering-R_k} corresponded to each one of {chest-R_k} in a regular one-to-one fashion, these time series of {steering-R_k} and {chest-R_k} were used to examine the reliability of heart rate variability of steering-ECG. There were 3 chest electrodes served by a (+) electrode on V5 of the left chest, a (-) electrode below the right clavicle, and an indifferent electrode below the left clavicle. This corresponded to lead II of a standard ECG. These electrodes were connected with an electrocardiograph (DPA-250S; Dia

Medical System Co., Tokyo; time constant = 1.5sec, low-pass filter of 0.7 – 30Hz). The signals were transferred to an AD converter and were sampled at 200Hz.

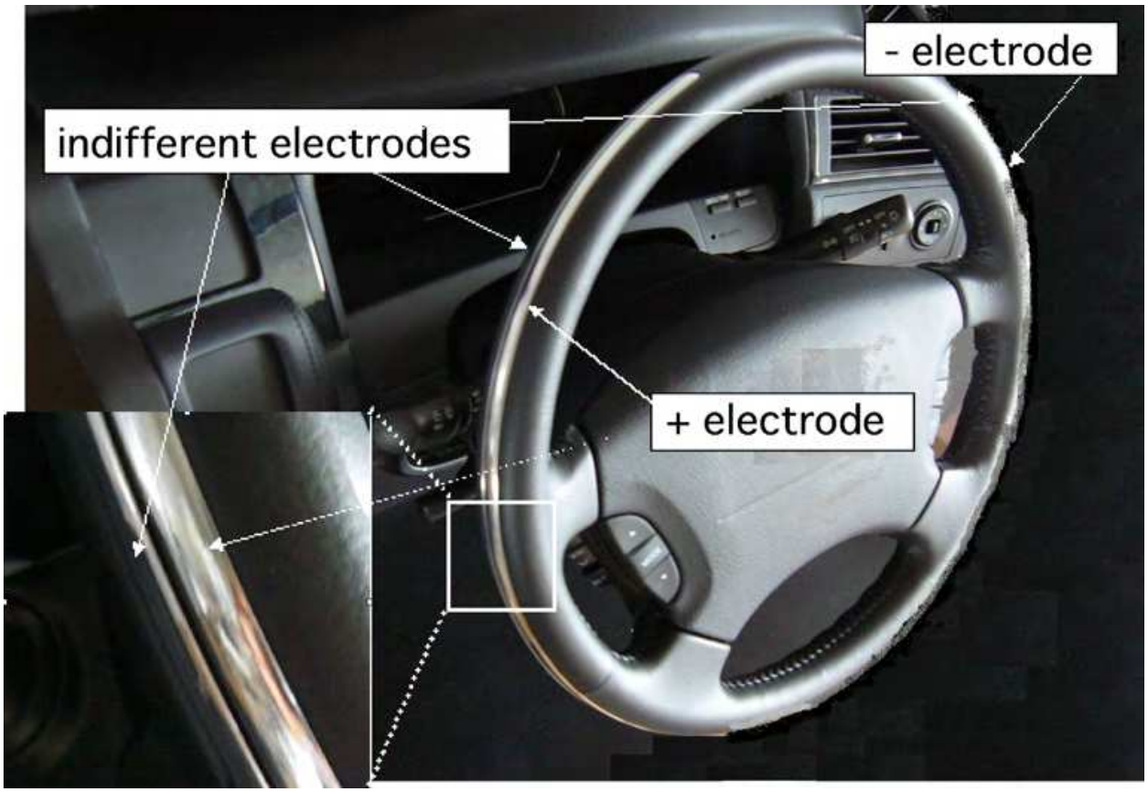

Fig. 5. A steering wheel. One pair of electrodes is installed around the grip site on each side. One of the two electrodes of each side is an indifferent electrode. The installed electrodes are arc-like (length 535mm, width 7mm, thickness 0.5mm) so that a driver can to some degree select a preferred grip site. From (Osaka et al., 2008).

2.2.3 Automated detection of QRS waves and measurement of RR intervals

The QRS waves were detected according to a flow chart, which we proposed newly (Figure 6). In a preliminary study, we examined the reliability of the algorithm by applying it to the electrocardiograms of the PhysioBank (Goldberger et al., 2000), which are freely available and downloadable digitized data (sampling rate 250Hz). Our algorithm could detect not only normal QRS waves but also abnormal QRS waves shown in Figure 7. After detecting QRS waves, the RR intervals, $\{I_n\}$, were measured as the intervals of peaks of two successive QRS waves. As the subjects sitting in the driver's seat did not remain still, outliers of RR intervals were always observed. Outliers were excluded as follows: 1) calculation of the MI and SDI (the mean value and standard deviation of $\{I_n\}$); 2) exclusion of outliers as I_n > MI + 2SDI or < MI - 2SDI, and representation of those intervals remaining after exclusion of the outliers as $\{J_n\}$; 3) calculation of the standard deviation of $\{J_n\}$(expressed as the SDJ); 4) calculation of the median, $MedJ_n$, of a set consisting of eleven consecutive intervals, $\{J_{n-5}, J_{n-4}, \ldots, J_n, J_{n+1}, \ldots, J_{n+5}\}$ for each interval (indexed as J_n); 5) consecutive search of outliers as J_n > $MedJ_n$ + SDJ or < $MedJ_n$ – SDJ; and 6) replacement of each of the outliers by $MedJ_n$ so that the intervals after the replacement could be regarded as RR intervals, $\{RRI_n\}$.

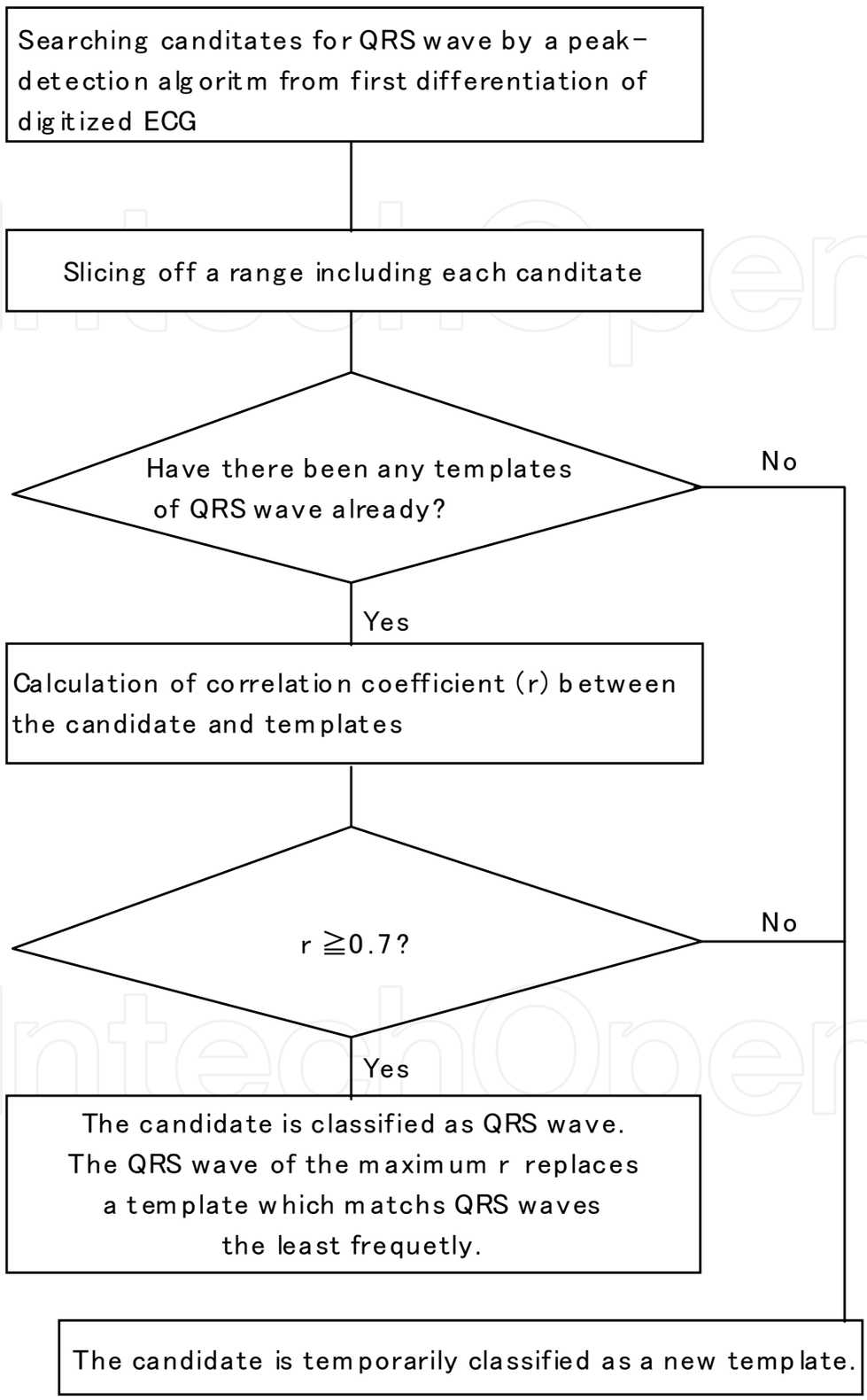

Fig. 6. A flow chart to detect QRS waves. From (Osaka et al., 2008).

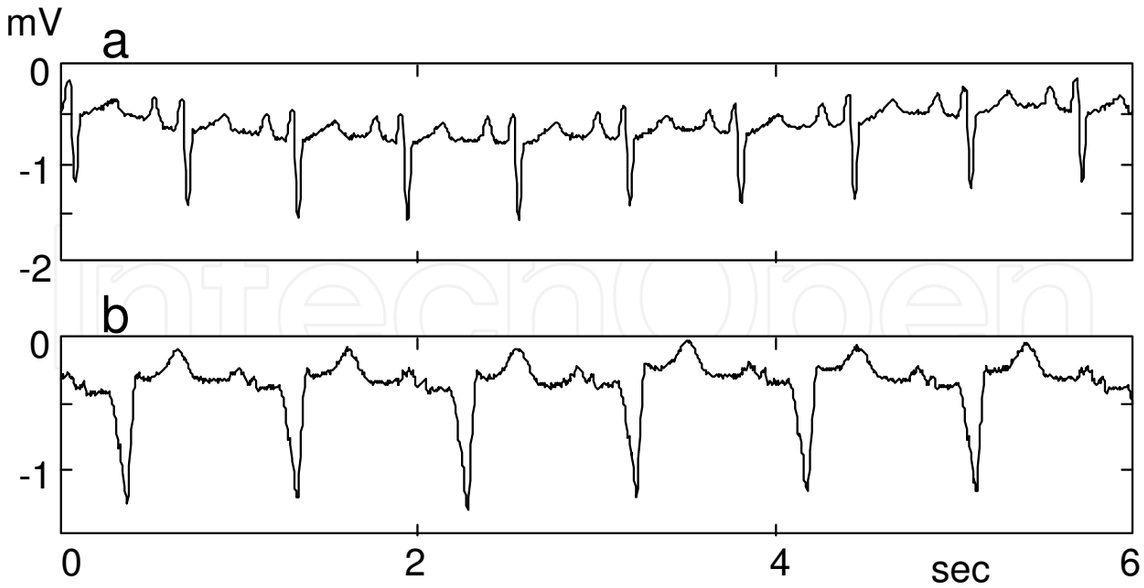

Fig. 7. Samples from the ECG database of PhysioBank. **a**, rS type. **b**, QS type.

2.2.4 Frequency analysis

A smoothed instantaneous heart rate time series was constructed from the RR-intervals and sampled at 8 Hz, according to Berger's method (Berger et al., 1986). The data length of an epoch was 64 sec. The confidence in spectral estimates could be enhanced by dividing the data into 5 epochs and by ensemble averaging of Welch's method (Bendat & Piersol, 1986). To reduce the loss of stability, the data were divided using a 50% overlap. Linear trends were removed from the data, and the data were tapered by use of a Hanning window. Then, a fast Fourier algorithm was used. We calculated the low-frequency component (LF: 0.04 - 0.15Hz) as a parameter of combined sympathetic and parasympathetic activity, the high-frequency component (HF: 0.15 - 0.40Hz) as that of parasympathetic activity, the ratio LF/HF as that of sympathetic activity, for each epoch. The natural logarithms of LF, HF, LF/HF, namely, ln(LF), ln(HF), and ln(LF/HF), were used to make these distributions approximate to normal distribution (Berger et al., 1989). The entire length of one record of ECG was 90 min, the data length of one epoch was 64 sec, and 2 consecutive epochs were overlapped by 50%. Hence, the total number of epochs was at most 168 (≈ 90min/32sec).

Since the subjects sitting in the driver's seat did not remain still and sometimes gripped a steering-wheel by only a single hand, more artifacts appeared in the steering-ECG than in the chest-ECG so that normal QRS waves were not recorded frequently. Hence, we took two steps to examine the reliability of heart rate variability of steering-ECG. Firstly, we compared ln(LF), ln(HF), and ln(LF/HF) of {steering-RR_k} with those parameters of {chest-RR_k}, because {steering-R_k} corresponded in a regular one-to-one fashion with {chest-R_k}. Each pair of R_k of {chest-R_k} and {steering-R_k} was consecutively searched visually on a screen. We would able to examine the reliability of the hardware system by the first step. The correlation coefficients between chest-ECG and steering-ECG for each parameter were calculated. The correlation coefficients were considered significant at $P<0.05$. Secondly, it was necessary to examine the reliability of the automated detection of QRS waves and measurement of RR intervals for practical use of our present system. According to the

algorithm, the outliers in $\{I_n\}$ of steering-ECG were more frequently replaced by $MedJ_n$ than those in $\{I_n\}$ of chest-ECG. We examined whether ln(LF), ln(HF), and ln(LF/HF) of steering-ECG were reliable in spite of such a disadvantage. We calculated the moving average of subsequent 5 epochs for ln(LF), ln(HF), and ln(LF/HF), and instantaneous heart rate (HR): m-ln(LF), m-ln(HF), m-ln(LF/HF), and m-HR. We constructed a time series of 4 parameters for chest-ECG and steering-ECG.

2.2.5 Mutual information

We drew graphs of fluctuations of m-ln(LF), m-ln(HF), m-ln(LF/HF), and m-HR for chest-ECG and steering-ECG. In order to compare the fluctuation of each parameter of steering-ECG with that of chest-ECG, we calculated the mutual information between them. This mutual information method was used to gauge the likeness between them. We calculated mutual information values, according to an algorithm proposed by Fraser and Swinney (Fraser & Swinney, 1986) and our previous study (Osaka et al., 1998). For a couple of time series, {x(t)} and {y(t)}, we measured how dependent the values of y(t) were on the values of x(t). We made the assignment [s,q] = [x(t), y(t)] to consider a general coupled system (S,Q). For example, {x(t)} was the time series of moving averages of m-ln(LF) for chest-ECG and {y(t)} was the time series of moving averages of m-ln(LF) for steering-ECG. Mutual information is defined as the answer to the question, "Given a measurement of s, how many bits on the average can be predicted about q?":

$$I(S,Q) = \int P_{sq}(s,q)\, log[P_{sq}(s,q)/(P_s(s)P_q(q))]dsdq,$$

where i) S and Q denote the systems, ii) $P_s(s)$ and $P_q(q)$ are the probability densities at s and q, respectively, and iii) $P_{sq}(s, q)$ is the joint probability density at s and q. The data length is 2^n. The algorithm is as follows: 1) an x-y plot is normalized into a square: each value W_i (= x(t) or y(t)) was replaced by an integer N_i; $1 \le N_i \le 2^n$; if $W_i < W_j$, $N_i < N_j$; if $W_i = W_j$ and $i < j$, $N_i < N_j$, so that each of the values of {x(t)} and {y(t)} is one to one replaced by an integer from 1 to 2^n, 2) it is successively divided into smaller squares, 3) a value for the dependence of y(t) on x(t) is calculated in each square, and 4) mutual information is the average of those values weighted by respective areas. Even if there is no significant correlation in the entire square, any significant correlation in smaller squares is taken into the final correlation by weighting by the respective areas. Therefore, mutual information is considered to be applicable more generally than a correlation coefficient of regression analysis. The larger is the value of mutual information for (S,Q), the stronger is the mutual dependence between S and Q. The data length was 2^7 (= 128). If S = Q, the correlation between them should be perfect. Then, I(S,Q) = n, where the data length is 2^n, because the algorithm is developed to the discrete case (Fraser & Swinney, 1986). The mutual information value between the same two time series is n. Hence, mutual information values were normalized by n, that is, these values were divided by n, resulting in values between 0 and 1. If the mutual information value was larger than or equal to 0.047, the correlation was taken to be strongly correlated on the basis of our previous report (Osaka et al., 1998).

2.3 Results

2.3.1 Results on the hardware system

Although small high-frequency noise still contaminated the baseline, the reproduced signals demonstrated the characteristics of P, R, and T waves well (Figure 8)). Each steering-ECG R

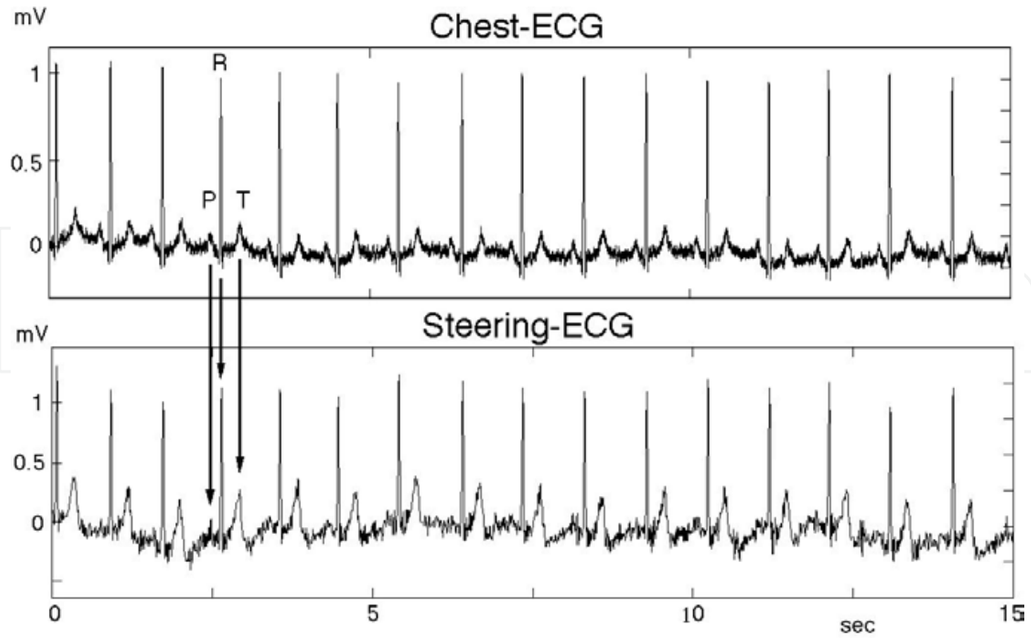

Fig. 8. Comparison of the electrocardiogram recorded from a steering wheel (steering-ECG) with that from a chest lead (chest-ECG). From (Osaka et al., 2008).

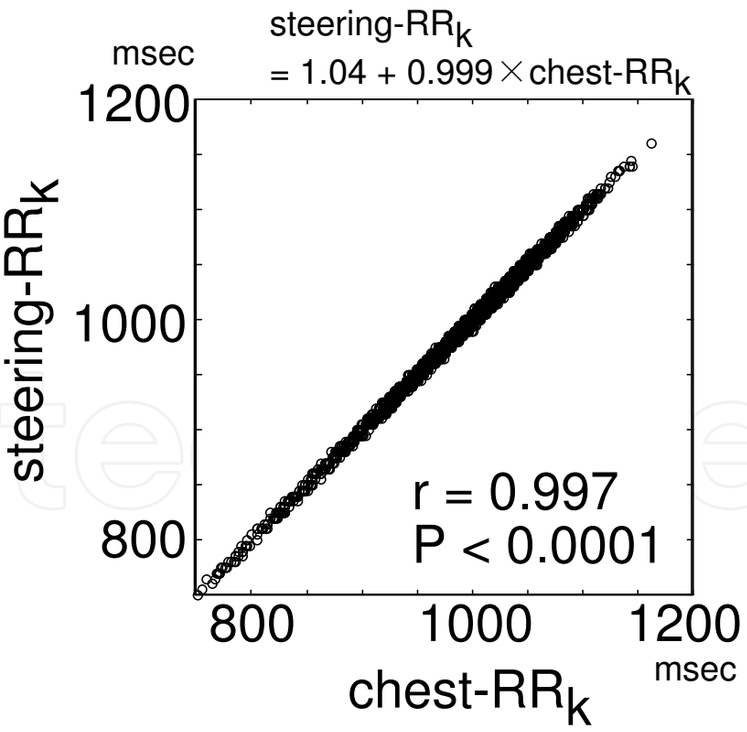

Fig. 9. A regression graph of steering-RR_k to chest-RR_k in the same subject as in Figure 8. Each element of {steering-R_k} corresponds to each one of {chest-R_k} in a regular one-to-one fashion by consecutively searching the R waves of the steering-ECG and chest-ECG visually on a screen. From (Osaka et al., 2008).

wave showed time-consistency with the respective R wave of the chest-ECG during the handling of a steering wheel as well as during the sitting still in the driver's seat. Figure 9 shows a regression graph of steering-RR_k to chest-RR_k in one of the subjects: steering-RR_k = 1.04 + 0.999×chest-RR_k (r = 0.997, P<0.0001). Hence, {steering-RR_k} was almost perfectly consistent with {chest-RR_k}. Similarly, the other subjects showed such a perfect consistency. For each parameter of ln(LF), ln(HF), and ln(LF/HF), a regression graph of steering-ECG (Y) to chest-ECG (X) was in the following: Y = a + b×X (-0.012≦a≦0.043, 0.997≦r≦1.000, P<0.0001) in all the subjects. ln(LF), ln(HF), and ln(LF/HF) of steering-ECG were almost perfectly consistent with those of chest-ECG.

2.3.2 Results on the software system

Figure 10 shows RR intervals from steering-ECG and from chest-ECG for the same subject as in Figure 8. When the driver moved his (her) upper body abruptly, the baseline of the chest-ECG fluctuated so that, intermittently, the R waves could not be detected. Hence, rather long erroneous RR intervals sometimes appeared in the tachogram of the chest-ECG as well as the steering-ECG. Longer RR intervals were observed more frequently in the tachogram of steering-ECG. This occurred because the driver sometimes gripped only one side of the steering wheel with a single hand. Since more long erroneous RR intervals were deleted in

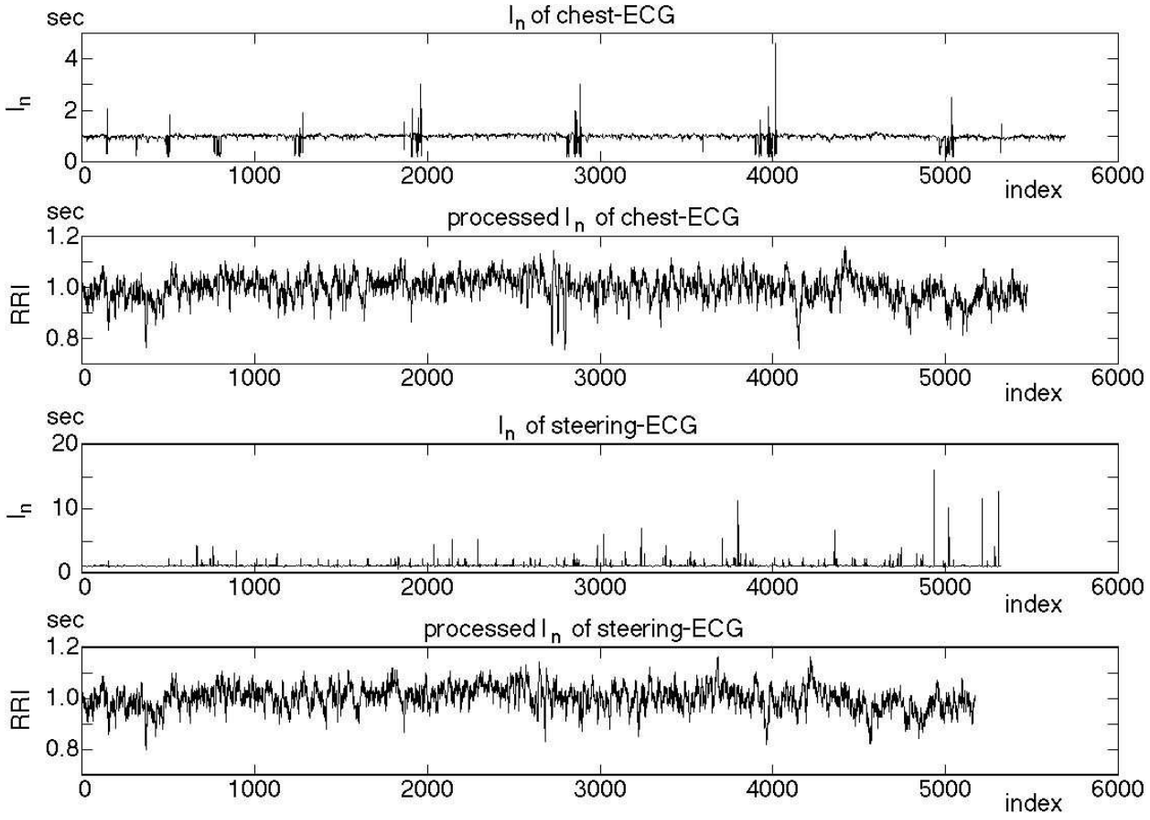

Fig. 10. RR intervals from steering-ECG and from chest-ECG for the same subject as in Fig. 8. $\{I_n\}$: intervals of peaks of two successive QRS waves. $\{RRI_n\}$: intervals regarded as RR intervals after the processing of outliers from $\{I_n\}$ by the algorithm. From (Osaka et al., 2008).

the steering-ECG than in the chest-ECG, the last index number of processed I_n of steering-ECG, {steering-RRI_n}, was smaller than that of processed I_n of chest-ECG, {chest-RRI_n} (Figure 10). Hence, each element of {steering-RRI_n} did not correspond in a regular one-to-one fashion with that of {chest-RRI_n} so that {steering-RRI_n} and {chest-RRI_n} could not be compared by the regression analysis. Figure 11 shows that the fluctuation from the steering-ECG resembled that from the chest-ECG for each parameter of the same subject as in Figure 8. Particularly, most of upslopes and downslopes of each parameter of steering-ECG corresponded one to one with those of chest-ECG. These findings were seen in the other subjects, when mutual information values were larger than 0.047. Figure 12 shows that mutual information of each parameter was larger than 0.047 with 95% confidence. Hence, it indicated that the fluctuation of each parameter of steering-ECG significantly resembled that of chest-ECG. However, the mutual information of m-ln(HF) in one subject and that of m-ln(LF/HF) in another were both 0. Mutual information values were all larger than 0.047 except for these 2 values.

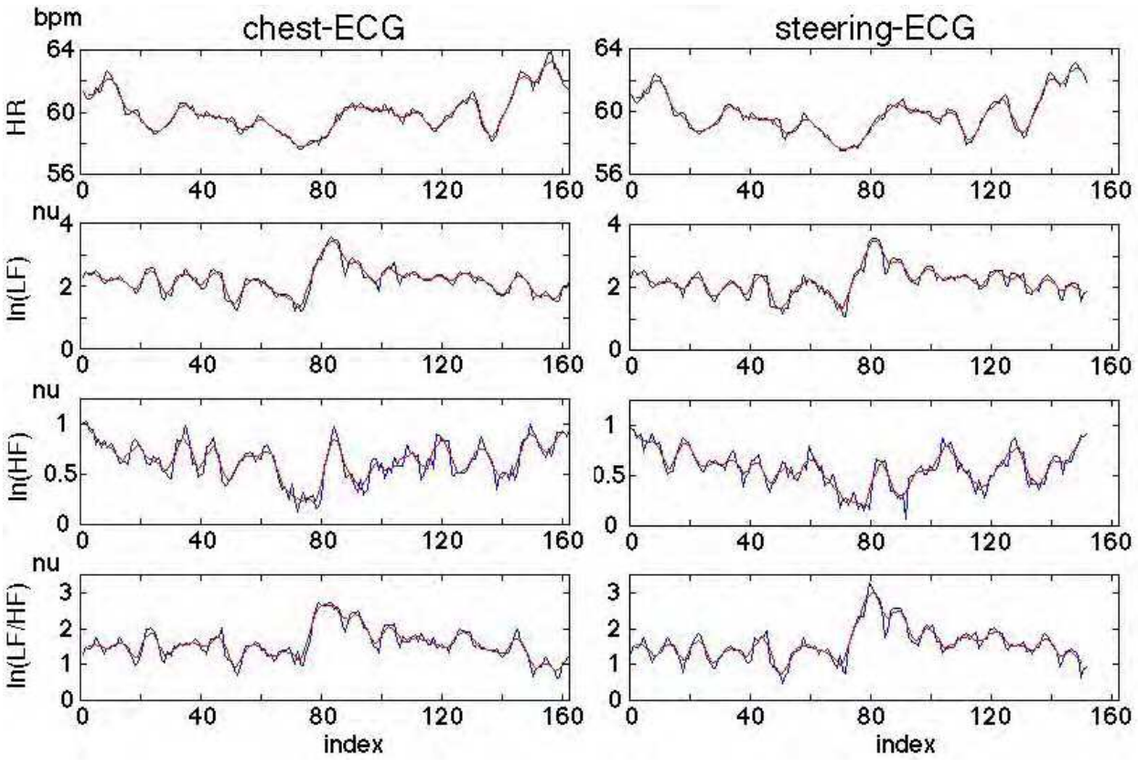

Fig. 11. Comparison of a fluctuation from steering-ECG with that from chest-ECG for each parameter of the same subject as in Figure 8. Red lines show the moving averages of blue lines. Mutual information values are 0.225, 0.223, 0.209, and 0.184 for m-HR, m-ln(LF), m-ln(HF), and m-ln(LF/HF). HR, heart rate; LF, low-frequency component (0.04 - 0.15Hz); HF, high-frequency component (0.15 - 0.40Hz); LF/HF, the ratio of LF to HF. ln(LF), ln(HF), and ln(LF/HF): natural logarithms of LF, HF, and LF/HF. m-HR, m-ln(LF), m-ln(HF), and m-ln(LF/HF): moving averages of HR, ln(LF), ln(HF), and ln(LF/HF). From (Osaka et al., 2008).

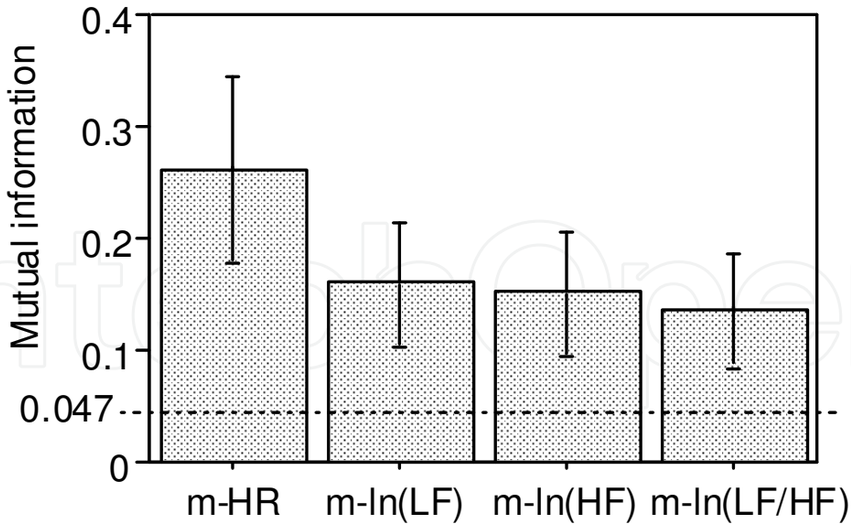

Fig. 12. Mean and 95%-confidence error bar of mutual information of m-HR, m-ln(LF), m-ln(HF), and m-ln(LF/HF). Threshold of significance: 0.047. HR, heart rate; LF, low-frequency component (0.04 - 0.15Hz); HF, high-frequency component (0.15 - 0.40Hz); LF/HF, the ratio of LF to HF. ln(LF), ln(HF), and ln(LF/HF): natural logarithms of LF, HF, and LF/HF. m-HR, m-ln(LF), m-ln(HF), and m-ln(LF/HF): moving averages of HR, ln(LF), ln(HF), and ln(LF/HF). From (Osaka et al., 2008).

2.4 Confirmation of correctness of steering ECG

The waves of P, Q, R, S, and T are generally visible clearly in a standard ECG, while a subject lies on the supine position. In the present study, the waves of P, R, and T could be recorded clearly in steering-ECG (Figure 8). {steering-RR_k} was almost perfectly consistent with {chest-RR_k} in all the subjects. Similarly, ln(LF), ln(HF), and ln(LF/HF) of steering-ECG were almost perfectly consistent with those of chest-ECG. Hence, the first half of our goals was achieved, using the following technical measures. The long indifferent electrodes were installed into both sides of the steering wheel so as to work without fail even if the driver's hands should move on the steering wheel. The electrodes installed into the steering wheel were made of plating to increase electrical conductivity. A bandpass filter of 0.2 ~35Hz was used for steering-ECG. It may be compared with the generally used bandpass filter of an electrocardiograph. Hence, the waves P, R, and T of the steering-ECG rather resembled those of chest-ECG. Small high-frequency noise contaminated not only the baseline of the steering-ECG but also that of the chest-ECG (Figure 8), indicating that it is difficult to record noise-free ECG in an automobile. This contaminating noise resulted from alternating current, making the ST-segment of the ECG unclear. Generally, small P waves, flat T waves, and small inverted T waves may be invisible by the contaminating noise. In order to detect ischemic attacks, namely, angina pectoris and acute myocardial infarction, it is necessary to eliminate that noise. We will endeavor to reduce noise in a further study.

After detecting QRS waves by our algorithm shown in Figure 6, we measured RR-intervals by using a peak-detection algorithm. In the preliminary study, we examined the reliability of this algorithm by applying to the ECG database of PhysioBank. It was applicable to the ECG of patients with abnormal Q waves in lead I, usually observed in broad anterior myocardial infarction or dilated cardiomyopathy (Figure 7) as well as the ECG of normal

subjects. When a driver moved his or her upper body abruptly and/or gripped only one side of the steering wheel with a single hand, normal R waves could intermittently not be detected, and long erroneous RR intervals appeared. Heart rate variability mainly results from the pacemaker sinus node rhythm, which is under the control of the autonomic nervous system. Therefore, a time series including frequent noisy RR intervals, for example, in subjects at high risk of lethal arrhythmia who have frequently premature beats, atrial tachyarrhythmia such as atrial fibrillation, or pace maker implantation is unsuitable for heart rate variability analysis. Practically, arrhythmias such as premature beats sometimes appear in even normal subjects, which cause erroneous RR intervals. Although the Task Force of the European Society of Cardiology and the North American Society of Pacing and Electrophysiology published a report about standards of measurement for heart rate variability in 1996, no standard for how to deal with such noisy RR intervals was included in the report. In subjects with frequent premature beats, the values of LF, HF, and LF/HF are rather inaccurate for data epochs including more premature beats. Thus, we presume that a method of dividing the data into 5 epochs with a 50% overlap and ensemble averaging is useful to enhance the confidence of those values, according to Welch's method (Bendat & Piersol, 1986).

Rather long or short RR intervals were excluded as outliers: I_n > MI + 2SDI or < MI - 2SDI. Consequently, about 5% of all the intervals I_n were excluded. These outliers resulted from artifacts due to abrupt body movement and/or gripping only one side of the steering wheel. More long erroneous RR intervals appeared in steering-ECG than in chest-ECG, and more outliers were excluded in steering-ECG. The number of RR intervals was less in steering-ECG than in chest-ECG (Figure 10). Each element of {steering-RRI_n} did not correspond in a regular one-to-one fashion with that of {chest-RRI_n} so that {steering-RRI_n} and {chest-RRI_n} could not be compared by the regression analysis. Hence, we needed the mutual information method as an alternative one in order to compare heart rate variability of {steering-RRI_n} and {chest-RRI_n}.

We aimed at drawing a reliable graph following a fluctuation of autonomic nervous activity. Mutual information of each parameter was larger than 0.047 with 95% confidence. This indicated statistically that the fluctuation of each parameter of steering-ECG significantly resembled that of chest-ECG. In detail, all but 2 mutual information values were larger than 0.047: mutual information of ln(HF) in one subject and that of ln(LF/HF) in another were 0. When these values of mutual information were 0, the fluctuations of steering-ECG did not seem to resemble the respective fluctuations of chest-ECG, since the steering-ECG was noisy due to the frequent gripping of a steering wheel by a single hand. We succeeded in demonstrating a fluctuation in autonomic nervous activity from steering-ECG, which was statistically consistent with that of chest-ECG. It is possible for a driver to observe a fluctuation of sympathetic nervous activity by ln(LF/HF) and a fluctuation of parasympathetic nervous activity by ln(HF). Hence, drivers can detect their own autonomic stress continuously. Atrial or ventricular premature beats can be detected by the present algorithm.

3. Addition of information from plethysmogram

Although the chest-ECG was recorded simultaneously as a reference in order to examine the correctness of the steering-ECG, the chest-ECG was also unavoidably contaminated. Hence, it was impossible to continuously find a one-to-one correspondence between the R waves of a

steering-ECG and those of a chest-ECG. We recorded plethysmogram as well as ECG from the steering wheel in order to compromise such missing recordings of ECG. Blood pressure is also very important information on physiological conditions. We examined whether various cardiac abnormalities could be detected reliably by ECG and plethysmogram recorded from the steering wheel. We aimed at making a robust system for monitoring a driver's physical conditions against noise and providing reliable information to the driver by integrating information from the steering-ECG and that from the plethysmogram for safety driving.

3.1 Subjects & methods

Forty-six subjects were evaluated: 9 normal volunteers and 37 patients (hypertension (N = 7), cardiomyopathy (N = 7), atrial fibrillation (N = 7), myocardial infarction (N = 6), valvular disease (N = 6), angina pectoris (N = 4)). Of these subjects, 8 showed ST depression, 4 left bundle block, 4 right bundle block, 4 low voltage, and 2 pacing rhythm of a implanted pacemaker.

We installed a sensor of a transmitted green photoelectric plethysmogram to detect the variation of arterial concentration of hemoglobin by reflection (bandpass-filter 0.2 ~ 5 Hz with reduction of 3 dB, sampling rate 1 kHz) into the steering wheel. Since the absorption rate of green by hemoglobin was higher than that of infra-red, which is used generally, the signal-to-noise ratio (S/N ratio) of the former was better than the latter so that plethysmogram could be recorded at the palm near the right thumb. The sensor was set up to touch the palm near the right thumb naturally, while the driver grips the steering wheel into which the electrodes for ECG were installed. To compare with those recordings from the steering wheel, we recorded ECG from a chest lead and plethysmogram directly from a finger simultaneously while they were sitting on the driving seat of the simulator for 10 minutes (Figure 13). We calculated the second derivative of plethysmogram as the

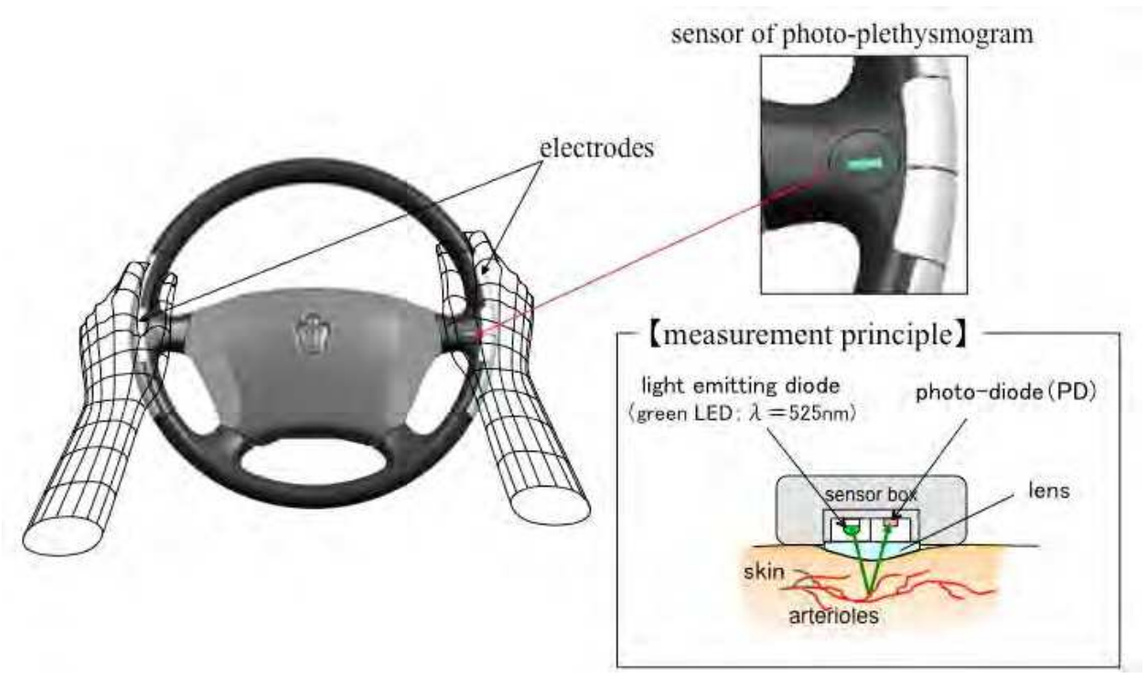

Fig. 13. Electrodes for electrocardiogram & a sensor for photo-plethysmogram.

acceleration of pulse wave. The positive component (a-wave) and the following negative component (b-wave) represent the forward component of systolic blood pressure (Figure 14) (Chua et al., 2010). Therefore, we presumed that the total amplitude of a-wave and b-wave reflects the strength of ejection in systole. The data of ECG and plethysmogram recorded from the steering wheel were stored in a hard disk, which were analyzed to obtain RR intervals and the second derivative of plethysmogram.

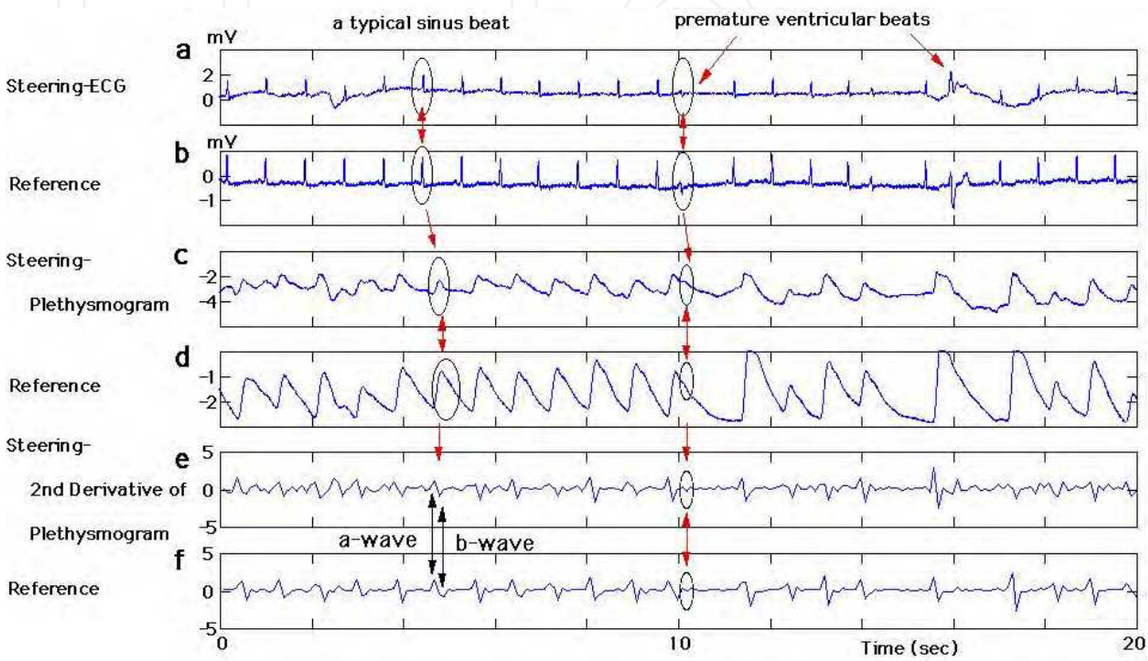

Fig. 14. An example of steering-electrocardiogram and plethysmogram.

3.2 Results

Figure 14 shows an example of steering-ECG, steering-plethysmogram and steering-second derivative of plethysmogram, comparing with the reference recordings. Each of QRS wave of the steering-ECG was consistent with that of the reference. Each of pulse wave of the steering-plethythmogram was consistent with that of the reference. Similarly, each pair of a-wave and b-wave of the steering-second derivative of plethysmogram was consistent with that of the reference. We could discriminate sinus bradycardia, sinus tachycardia, and atrial fibrillation by measuring RR-intervals. We could also discriminate premature ventricular beats and premature atrial beats by measuring the timing and width of QRS and by plethysmogram, which was particularly useful because premature ventricular beats caused only a minute pulse wave (Figure 14c, d) and premature atrial beats caused almost normal pulse waves. Since only a minute blood volume is outputted by premature ventricular beats, a-wave and b-wave did not appear (Figure 14e, f). When a subject did not grip the steering wheel normally, the recordings of ECG were sometimes contaminated by noise, such as a fluctuation of the baseline. Figure 15 shows that beat-to-beat intervals can be calculated from the steering-plethysmogram and/or the steering-second derivative of it, in case a large fluctuation of the baseline hinders the calculation of RR intervals. If plethysmogram was

recorded normally, such missing RR intervals of the steering-ECG could be replaced by peak intervals of plethysmogram. Figure 14 shows that ST depression can be observed in the steering-ECG like the reference. Thus, ST changes could be detected without such a large fluctuation of the baseline.

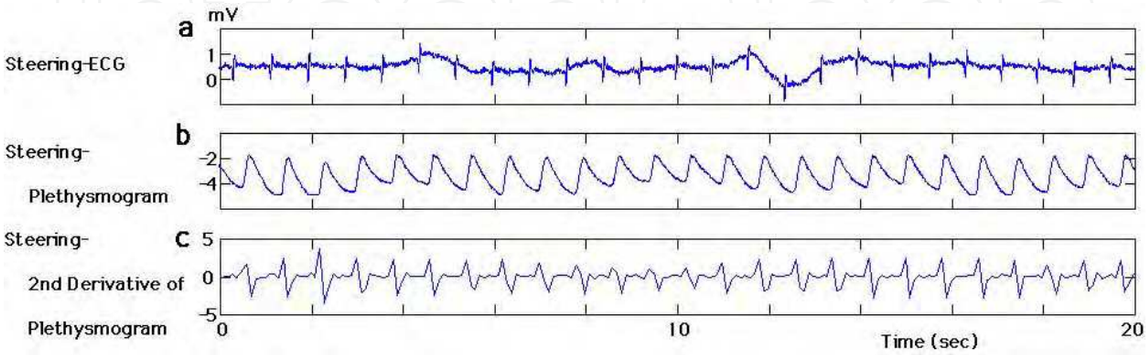

Fig. 15. An example of fluctuaion of the baseline of steering-electrocardiogram.

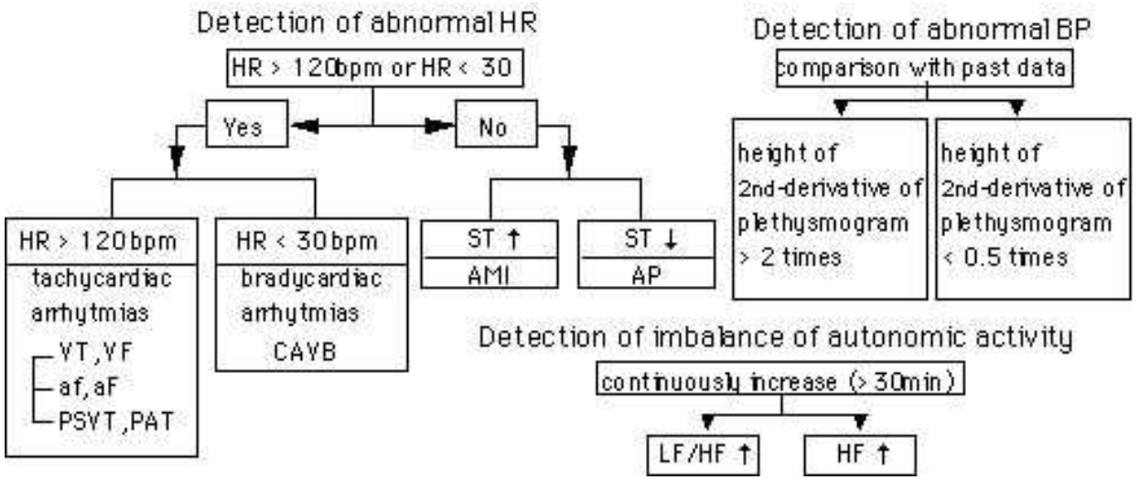

Fig. 16. Flow chart to detect abnormal physiological conditions. HR, heart rate; bpm, beats per minute; BP, blood pressure; VT, ventricular tachycardia; VF, ventricular fibrillation; af, atrial fibrillation; aF, atrial flutter; PSVT, paroxysmal supraventricular tachycardia; PAT, paroxysmal atrial tachycardia; CAVB, complete atrioventricular block; AMI, acute myocardial infarction; AP, angina pectoris; LF, low-frequency component of heart rate variability; HF, high-frequency component.

4. Conclusion

In order to improve the reliability of the system to detect abnormal physiological conditions while driving and make it more applicable, we installed the sensor of photo-plethysmogram besides the electrodes of ECG into the steering wheel. We demonstrated that RR intervals calculated from the steering-ECG and the graph following a fluctuation of autonomic activity were consistent with those obtained from the reference-ECG. It is possible for a driver to observe a trend of heart rate, a fluctuation of sympathetic activity by ln(LF/HF), and a fluctuation of parasympathetic activity by ln(HF) on a monitor of navigation. Hence, drivers can check whether arrhythmia appears or not, and their own autonomic stress continuously and easily. Similarly, we showed that the plethysmogram of the steering wheel and the second derivative of it were consistent with those from the reference. In a stable condition such as sitting on a driving seat, HR > 120 beats/min (bpm) and HR < 30 bpm are considered to be abnormal so that the driver is possibly at risk from causing a traffic accident (Figure 16). When the height of a-wave plus b-wave of the second derivative of plethysmogram is >2 times larger than the mean value of it for the previous 30 minutes or <0.5 times smaller, blood pressure is considered to increase or decrease abruptly. When LF/HF or HF is increasing steadily for >30 minutes, it will indicate that sympathetic activity may predominate over parasympathetic activity excessively or vise versa (Figure 16). If these abnormalities are detected, a message of inquiring of the driver, "Are you all right?" will be delivered in our system. If the driver needs any help, some of the nearest hospitals will be displayed on the screen of the navigation system. This hospital-referring system has already installed into automobiles of a high grade of TOYOTA MOTOR CORPORATION. A network system by which the data is continuously transferred to a center and monitored by medical doctors will be made in the near future. We will call it the human-machine talking system. We propose such a new system by which it is monitored whether physiological conditions are within a normal state of the driver or not. To decide it, the present data of heart rate, the height of a-wave plus b-wave, LF/HF and HF are continuously compared with those parameters from the past data of the driver. Hence, we call it a customized heart check system. Feedback of information to the driver on autonomic stress and the appearance of premature beats will improve safety. Our system will open doors to new strategies to minimize driver's risk by making available the relevant data during the actual process of driving. We reported that a V-shaped trough in autonomic activity is a possible precursor of life-threatening cardiac events (Osaka et al., 2010). The V-trough including the small variations that precede it spans approximately 190 minutes. Hence, a necessary condition for the detection of the precursor with our algorithm is that the time from the start of recording to an event must exceed 190 minutes. Thus the somewhat lengthy recording time required is a potential shortcoming of the system. Therefore, the detection of the V-shaped trough is considered to be useful for subjects who drive for long hours, especially professional drivers of bus, taxi, and truck. This system will be also useful to monitor physiological conditions of a man or woman at home as well as an inpatient, for example if the system is installed into the bed. If it is installed into a toilet stool, physiological conditions will be easily checked up daily.

5. Acknowledgement

This study was done in cooperation with Minoru Makiguchi (TOYOTA MOTOR CORPORATION), Tsuyoshi Nakagawa, Taiji Kawachi, Kazuhiro Sakai and Shinya

Matsunaga (DENSO), Hiroshi Hayashi, M.D., Hiroshige Murata, M.D., and Takao Katoh, M.D. (Nippon Medical School).

6. References

Bauer, A.; Kantelhardt, J.W.; Barthel, P.; Schneider, R.; Mäkikallio, T.; Ulm, K.; Hnatkova, K.; Schomig, A.; Huikuri, H.; Bunde, A.; Malik, M. & Schmidt, G. (2006) Deceleration capacity of heart rate as a predictor of mortality after myocardial infarction: cohort study. *Lancet*, Vol.367, pp. 1674-1681

Bendat, J.S. & Piersol, A.G. (1986) *Random Data Analysis and Measurement Procedures* (2nd edition), Wiley, New York

Berger, R.D.; Akselrod, S.; Gordon, D. & Cohen, R.J. (1986) An efficient algorithm for spectral analysis of heart rate variability. *IEEE Transactions of Biomedical Engineering,* Vol.33, pp. 900-904

Berger, R.D.; Saul, J.P. & Cohen, R.J. (1989) Transfer function analysis of autonomic regulation I. Canine atrial rate response, *American Journal of Physiology (Heart Circulation Physiology)* Vol.256, pp. H142-H152

Chua, E.C., Redmond, S.J., McDarby, G. & Heneghan, C. (2010) Towards using photo-plethysmogram amplitude to measure blood pressure during sleep. *Annals of Biomedical Engineering*, Vol.38, pp. 945-954.

Fraser, A.M. & Swinney, H.L. (1986) Independent coordinates for strange attractors from mutual information. *Physical Review A*, Vol.33, pp. 1134-1140

Goldberger, A.L.; Amaral, L.A.N.; Glass, L.; Hausdorff, J.M.; Ivanov, P.C.; Mark, R.G.; Mietus, J.E.; Moody, G.B.; Peng, C.K. & Stanley, H.E. (2000) PhysioBank, PhysioToolkit, and PhysioNet: Components of a New Research Resource for Complex Physiologic Signals. *Circulation,* Vol.101, pp. e215-e220

Huikuri, H.V.; Valkama, J.O.; Airaksinen, K.E.; Seppanen, T; Kessler, K.M.; Takkunen, J.T. & Myerburg, R.J. (1993) Frequency domain measures of heart rate variability before the onset of nonsustained and sustained ventricular tachycardia in patients with coronary disease. *Circulation,* Vol.87, pp. 1220-1228

Ivanov, P.C.; Amaral, L.A.; Goldberger, A.L.; Havlin, S.; Rosenblum, M.G. Struzik, Z.R. & Stanley, H.E. (1999) Multifractality in human heartbeat dynamics, *Nature* Vol.399, pp. 461-465

Jeong; Lee, I.C.; Park, D.H.; Ko, S.W.; Yoon, J. & Ro, H. (2007) Automobile driver's stress index provision system that utilizes electrocardiogram, In: *Intelligent Vehicles Symposium*, pp. (652-656) IEEE, Istanbul, Turkey

Kobayashi, M. & Musha, T. (1982) 1/f fluctuation of heartbeat period. *IEEE Transactions of Biomedical Engineering* Vol.29, pp. 456-457

Lam, L.T. & Lam, M.K.P. (2005) The association between sudden illness and motor vehicle crash mortality and injury among older drivers in NSW, Australia. *Accident Analysis and Prevention,* Vol.37, pp. 563-567

Muller, J.E.; Ludmer, P.L.; Willich, S.N.; Tofler, G.H.; Aylmer, G.; Klangos, I. & Stone, P.H. (1987) Circadian variation in the frequency of sudden cardiac death. *Circulation*, Vol.75, pp131-138

Osaka, M.; Saitoh, H.; Atarashi, H. & Hayakawa, H. (1993) Correlation dimension of heart rate variability: a new index of human autonomic function, *Frontiers of Medical and Biological Engineering,* Vol.5, pp. 289-300

Osaka, M.; Saitoh, H.; Sasabe, N.; Atarashi, H.; Katoh, T.; Hayakawa, H. & Cohen, R.J. (1996) Changes in autonomic activity preceding onset of nonsustained ventricular tachycardia, *Annals of Noninvasive Electrocardiology,* Vol..1, pp. 3-11

Osaka, M.; Yambe, T.; Saitoh, H.; Yoshizawa, M.; Itoh, T.; Nitta, S. & Hayakawa, H. (1998) Mutual information discloses relationship between hemodynamic variables in artificial heart-implanted dogs. *American Journal of Physiology,* Vol.275, pp. H1419-H1433

Osaka, M. & Watanabe, M.A. (2004) A modified Chua circuit simulates *1/f*-fluctuation of heartbeat interval. *International Journal of Bifurcation and Chaos*, Vol.14, pp. 3449-3457

Osaka, M.; Murata, H.; Fuwamoto, Y.; Nanba, S.; Sakai, K. & Katoh, T. (2008) Application of heart rate variability analysis to electrocardiogram recorded outside the driver's awareness from an automobile steering wheel. *Circulation Journal,* Vol.72, pp. 1867-73

Osaka, M.; Watanabe, E.; Murata, H.; Fuwamoto, Y.; Nanba, S.; Sakai, K. & Katoh, T. (2010) V-Shaped Trough in Autonomic Activity is a Possible Precursor of Life-Threatening Cardiac Events. *Circulation Journal*, Vol.74, pp. 1906-1915

Osaka, M. (in press) A modified chua circuit simulates a v-shaped trough in autonomic activity as a precursor of sudden cardiac death. *International Journal of Bifurcation and Chaos*

Peng, C-K.; Mietus, J.; Hausdorff, J.M.; Havlin, S.; Stanley, H.E. & Goldberger, A.L. (1993) Long-range anticorrelations and non-Gaussian behavior of the heartbeat, *Physical Review Letters,* Vol.70, pp. 1343-1346

Routley, V.; Staines, C.; Brennan, C.; Haworth, N. & Ozanne-Smith, J. (2003) Suicide and Natural Deaths in Road Traffic – Review. *Monash University Accident Research Centre Report*, Vol.216

Sakata, K.; Kumagai, H.; Osaka, M.; Onami, T.; Matsuura, T.; Imai, M. & Saruta, T. (2002) Potentiated sympathetic nervous and renin-angiotensin systems reduce nonlinear correlation between sympathetic activity and blood pressure in conscious spontaneously hypertensive rats. *Circulation,* Vol.106, pp. 620-625

Schwartz, P.J.; Vanoli, E.; Stramba-Badiale, M.; De Ferrari, G.M.; Billman, G.E. & Foreman, R.D. (1988) Autonomic mechanisms and sudden death. New insights from analysis of barorecepor reflexes in conscious dogs with and without a myocardial infarction. *Circulation,* Vol.78, pp. 969-979

Task Force of the European Society of Cardiology and the North American Society of Pacing and Electrophysiology. (1996) Heart rate variability: Standards of measurement, physiological interpretation, and clinical use. *Circulation,* Vol.93, pp. 1043-1065

Taylor, J.A. & Eckberg, D.L. (1996) Fundamental relations between short-term RR interval and arterial pressure oscillations in humans. *Circulation,* Vol.93, pp. 1527-1532

Toyoshima, H.; Hayashi, S.; Tanabe, N.; Miyanishi, K.; Satoh, T.; Aizawa, Y. & Izumi, T. (1996) Sudden death of adults in Japan. *Nagoya Journal of Medical Science,* Vol.59, pp. 81-95

Zipes, D.P. & Wellens, H.J. (1998) Sudden cardiac death, *Circulation*, Vol.98, pp. 2334-2351

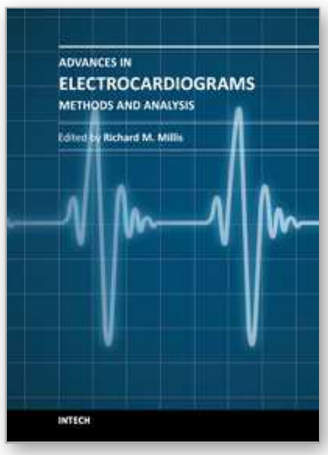

Advances in Electrocardiograms - Methods and Analysis
Edited by PhD. Richard Millis

ISBN 978-953-307-923-3
Hard cover, 390 pages
Publisher InTech
Published online 25, January, 2012
Published in print edition January, 2012

Electrocardiograms are one of the most widely used methods for evaluating the structure-function relationships of the heart in health and disease. This book is the first of two volumes which reviews recent advancements in electrocardiography. This volume lays the groundwork for understanding the technical aspects of these advancements. The five sections of this volume, Cardiac Anatomy, ECG Technique, ECG Features, Heart Rate Variability and ECG Data Management, provide comprehensive reviews of advancements in the technical and analytical methods for interpreting and evaluating electrocardiograms. This volume is complemented with anatomical diagrams, electrocardiogram recordings, flow diagrams and algorithms which demonstrate the most modern principles of electrocardiography. The chapters which form this volume describe how the technical impediments inherent to instrument-patient interfacing, recording and interpreting variations in electrocardiogram time intervals and morphologies, as well as electrocardiogram data sharing have been effectively overcome. The advent of novel detection, filtering and testing devices are described. Foremost, among these devices are innovative algorithms for automating the evaluation of electrocardiograms.

How to reference
In order to correctly reference this scholarly work, feel free to copy and paste the following:

Motohisa Osaka (2012). Customized Heart Check System by Using Integrated Information of Electrocardiogram and Plethysmogram Outside the Driver's Awareness from an Automobile Steering Wheel, Advances in Electrocardiograms - Methods and Analysis, PhD. Richard Millis (Ed.), ISBN: 978-953-307-923-3, InTech, Available from: http://www.intechopen.com/books/advances-in-electrocardiograms-methods-and-analysis/customized-heart-check-system-by-using-integrated-information-of-electrocardiogram-and-plethysmogram

INTECH
open science | open minds

InTech Europe
University Campus STeP Ri
Slavka Krautzeka 83/A
51000 Rijeka, Croatia
Phone: +385 (51) 770 447
Fax: +385 (51) 686 166

InTech China
Unit 405, Office Block, Hotel Equatorial Shanghai
No.65, Yan An Road (West), Shanghai, 200040, China
中国上海市延安西路65号上海国际贵都大饭店办公楼405单元
Phone: +86-21-62489820
Fax: +86-21-62489821

IntechOpen

IntechOpen